

DEFECT ENGINEERING FOR IMPROVED PHOTOCATALYTIC PERFORMANCE OF REDUCED LEAD TITANATE (PbTiO₃) UNDER SOLAR LIGHT IRRADIATION

M. Hassan Farooq^{1,2*}, I. Aslam³, H. Sadia Anam², M. Tanveer⁴ and M. Rizwan⁵

¹Laboratory of Eco-Materials and Sustainable Technology, The Xinjiang Technical Institute of Physics and Chemistry, Chinese Academy of Sciences, Urumqi, Xinjiang 830011, China

²Basic Sciences and Humanities Department, University of Engineering and Technology, KSK Campus, Lahore, Pakistan

³Department of Basic Sciences and Humanities, University of Engineering and Technology, NWL Campus, Lahore, Pakistan

⁴Department of Physics, University of Lahore, Gujrat Campus, Pakistan

⁵Department of Physics, University of Gujrat, Gujrat, Pakistan

(Received October 29, 2018; Revised April 20, 2019; Accepted May 5, 2019)

ABSTRACT. Lead titanate (PbTiO₃) nanoparticles were prepared successfully by template free hydrothermal method. Size, crystallinity, morphology and phase determination of the nanoparticles were made by X-ray diffraction (XRD), energy dispersive X-ray spectroscopy (EDS) and field-emission scanning electron microscopy (FESEM). FESEM results had shown that all nanoparticles were in the range between 20 to 40 nm size and found in the form of agglomerates. The average crystallite size of PbTiO₃ nanoparticles was calculated to be nearly 35 nm. PbTiO₃ nanoparticles were reduced by hydrogenation at high temperature to make the material active for visible light. Furthermore, optical absorbance of PbTiO₃ nanoparticles was determined by applying ultraviolet-visible-near infrared (UV-Vis-NIR) spectroscopy. By using Davis-Mott model, the direct optical band gap of 2.65 eV was acquired. Methyl orange (MO) was used as pollutant to check the photocatalytic activity of reduced PbTiO₃ nanoparticles under solar light irradiation. Photocatalytic activity of reduced PbTiO₃ nanoparticles increased 2.6 times more than that of pure PbTiO₃ nanoparticles for methyl orange (MO) under solar light irradiation.

KEY WORDS: Lead titanate (PbTiO₃), Photocatalytic performance, Hydrothermal growth, Solar light, Irradiation

INTRODUCTION

Recently, efforts have been made for the progress of functional nanomaterials, which can introduce new opportunities for the development of functional nanostructures. Oxide based functional materials such as zinc oxide (ZnO) and titanium dioxide (TiO₂) has been investigated intensively for its various applications in chemical sensors, photocatalytic reactions, and energy conversion fields [1-4] because of their low cost advantages and non-toxicity. During the past few decades, TiO₂ has been considered as a photocatalyst for the degradation of organic pollutants for environmental applications after the discovery of decomposition of water into oxygen and hydrogen by Fujishma and Honda in 1972 for the first time [5].

A critical drawback of titania, however, is that it has a large band gap (3.2 eV), which limits its activity under UV light. UV light is only the 3-5% of solar light. Efforts have been made to tune the band gap of titania to make it responsive for visible light spectrum which is 50% of the solar light. Doping of metal and non-metal ions are considered as a strong tool for reducing the band gap of TiO₂ [6-10]. Metal ions with oxidation state less than Ti⁺⁴ such as B, Al, Sb, etc causes to produce the acceptor levels just above the valance band while doping of some non-metal ions such as carbon and nitrogen also causes to introduce the acceptor energy levels above the valance band. Doping of transition metal ions produces the energy levels just below the conduction band such as V⁺⁵, F⁻¹, etc [11, 12]. New energy states in the form of acceptor levels

*Corresponding author. mhfarooq@uet.edu.pk

This work is licensed under the Creative Commons Attribution 4.0 International License

or donor levels causes to reduce the band gap which extends the activity of TiO₂ for visible region. Another, technique for reducing the band gap of TiO₂ is to reduce the T⁺⁴ to Ti⁺³. Reduction of T⁺⁴ to Ti⁺³ produces a donor level just below the conduction band. To get complete control over the reduction of Ti⁺⁴ to Ti⁺³ is a great challenge for researchers. Mainly, hydrogenation of TiO₂ nanoparticles plays a key role for the reduction of Ti⁺⁴ to Ti⁺³ and produces black TiO₂ with band gap of nearly 1.54 eV [13] which is responsive under visible region of electromagnetic spectrum. Hydrogenation of TiO₂ is done under high temperature and pressure while hydrogen is highly flammable gas and it has limitations for industrial application of TiO₂.

More recently, composites of TiO₂ with low band gap materials were prepared and used for photocatalytic performance. Composites of TiO₂ with low band gap materials such as CdS, CdSe, CuO, CuS causes to improve the photocatalytic response under visible light irradiation and UV light [14-18]. Composites of such materials were prepared with different morphologies, core-shell structures, nano wires, nano tube, nano rods etc.

Another challenge, which reduces the performance of TiO₂, is its high electron-hole recombination rate which limits its activity. In order to inhibit the electron-hole recombination, TiO₂ is coated with p-type materials such as CuO, NiO, SnO [19-22], etc. These composites inhibit the electron-hole recombination rate and improve the photocatalytic performance of TiO₂ nanoparticles.

Titanates have been neglected for investigation of its photocatalytic performance because of its complex structure and large band gap. However, these have been studied for electrical, optical and piezoelectric properties [23, 24]. According to our knowledge, few reports have been published on SrTiO₃, ZnTiO₃, and FeTiO₃ for their photocatalytic properties [25, 26]. Meidan *et al.*, have reported the garden like superstructure of SrTiO₃ synthesized by hydrothermal method and showed super photocatalytic behavior for degradation of pollutant such as methyl blue (MB) [27]. Kong *et al.*, have reported the preparation of ZnTiO₃ powder and investigated the photocatalytic performance of the material [25]. We prepared PbTiO₃ by hydrothermal synthesis and tuned its band gap (2.65 eV) as low as responsive for visible light region by hydrogenation. In literature band gap of PbTiO₃ is reported from 3 eV to 4.5 eV [28, 29] experimentally while theoretically it is calculated upto 1.7 eV [30]. To the best of our knowledge, no single report has been published on photocatalytic performance of PbTiO₃ yet [27]. Moreover, we investigated the photocatalytic performance of PbTiO₃ nanoparticles for methyl orange (MO) under solar light.

EXPERIMENTAL

Sample preparation

Pure PbTiO₃ nanoparticles were prepared by template free hydrothermal method. Pb(OH)₂, Titanium tetra isopropoxide (TTIP), diethanol amine (DEA) and distilled water H₂O were used as preliminary materials. 40 mL of 0.45 M solution of Pb(OH)₂ was obtained by dissolving 4.3417 g Pb(OH)₂ under constant stirring for 10 min at 60 °C. Similarly, another 0.45 M solution of TTIP was prepared. The solution concentration is maintained at 0.5 M and the molar ratio is kept at 1.0 for diethanolamine (DEA) to titanium tetra isopropoxide (TTIP). Homogeneous mixture of these solutions was obtained by mixing and stirring these two solutions for two hours at room temperature. The Teflon lined stainless autoclave is used for the template free hydrothermal method by transferring the homogeneous solution inside the autoclave which is heated at 180 °C in oven for 24 hours. After the completion of reaction, the obtained precipitates were washed several times with the deionized water and ethanol through centrifuge, and then dried at 80 °C for 12 hours in oven. The prepared lead titanate nanoparticles were reduced by hydrogenation. White lead titanate powder was heated at 500 °C for three hours under the constant flow of hydrogen gas to get black colored powder.

Characterization

X-ray powder diffraction analysis was conducted on a Rigaku D/MAX-RB X-ray diffractometer (XRD), using CuK α radiation ($\lambda = 1.54056 \text{ \AA}$) to investigate the crystal structure of synthesized material. Morphological details of prepared samples were investigated by using field emission scanning electron microscopy (FE-SEM) (Zeiss-SUPRA55). Energy dispersive X-Ray Spectroscopy (EDX) equipped with FESEM was used to measure the elemental compositions of the synthesized material. Band gap of pure PbTiO₃ and reduced PbTiO₃ was measured by using UV-Vis spectro-photometer (Jasco V-570).

Photocatalytic activity

Photocatalytic performance of PbTiO₃ and reduced PbTiO₃ was measured by the degradation efficiency of methyl orange (MO) under solar light irradiation. For performing the photodegradation experiments, 50 mg samples of powder was suspended in 200 mL of 10 mg/L solution of MO in 250 mL reactor. A 500 Watt Xenon lamp was used as a source of solar light. Spectrophotometer is used to measure the UV-Visible absorption spectrum of the filtered solution. Area of adsorption band in the range of 200 to 800 nm was integrated to monitor the reaction process. Degradation of the pollutant at any time was analyzed and measured by C/C_0 where C_0 gives the maximum absorption intensity at zero time and C shows the absorption intensity at time “ t ”.

RESULTS AND DISCUSSION

Figure 1(a) depicts the XRD pattern of PbTiO₃ and reduced PbTiO₃ nano particles prepared by hydrothermal method. All the diffraction peaks of XRD graph, shown in Figure 1(a), are well matched to the tetragonal structure of PbTiO₃ (JCPD file # 06-0452). Good crystallinity of prepared material can be observed from the sharpness of the diffraction peaks. Furthermore, absence of any characteristic peak corresponding to the impurity ensures the purity of synthesized material. Debye-Scherrer formula [31] was used to measure the crystallite sizes of PbTiO₃ structure. The average crystallite size of synthesized materials is estimated to be 35nm.

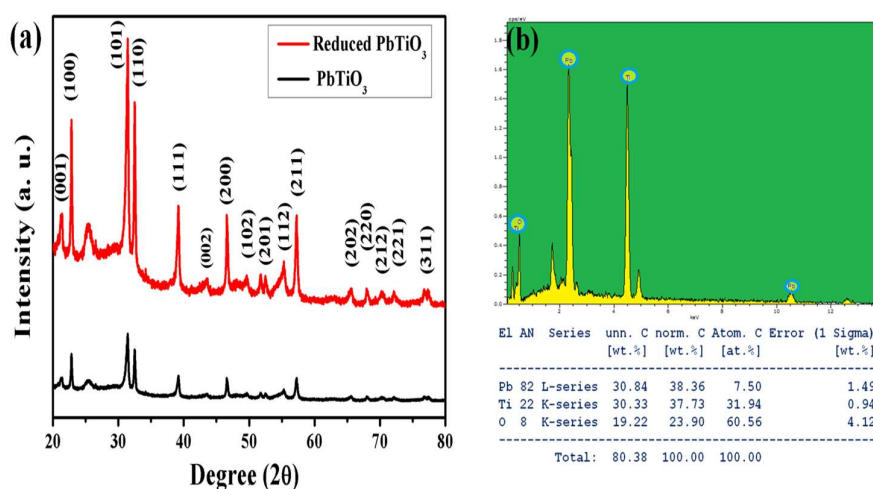


Figure 1. (a) XRD pattern of PbTiO₃ nanoparticles and (b) EDX spectra of PbTiO₃ nanoparticles.

Figure 1(b) shows the EDX pattern of PbTiO_3 nanoparticles. EDX graph confirms the presence of Pb, Ti and O elements. Absence of any impurity peak in the EDS patterns confirms the purity of synthesized material. Atomic weight percentage of Pb, Ti and O atoms confirms the formation of PbTiO_3 . Atomic weight ratio between Pb to Ti and O atoms is 1:1.02 and 1:3.4 respectively. As oxygen ratio is not taken accurate by EDX analysis due to experimental limitations.

Morphology of the nanoparticles is studied by field FESEM. Figure 2 represents the FESEM images of the PbTiO_3 and reduced PbTiO_3 nanoparticles synthesized by hydrothermal method. It can be observed that all the nanoparticles are in the size ranging from 20 to 40 nm. Figure 2(a-b) represent that all PbTiO_3 nanoparticles are in the form of agglomerates. Figure 2(c-d) represents the FESEM images of hydrogenated PbTiO_3 nanoparticles which are also in the form of agglomerates but little dispersed as compared to PbTiO_3 prepared by template free hydrothermal method and in the range of 20 to 40 nm.

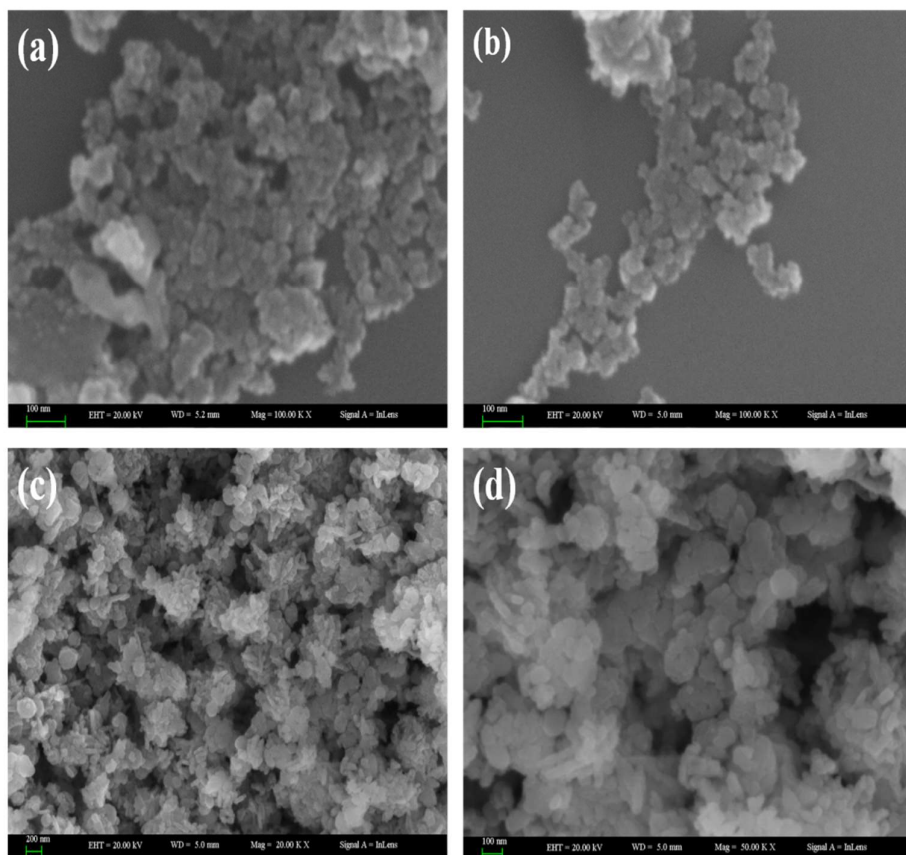


Figure 2. FESEM images of PbTiO_3 nanoparticles.

Figure 3(a) shows the UV-visible absorption spectrum for reduced PbTiO_3 nanoparticles. It can be observed from the UV-graph that PbTiO_3 nanoparticles shows absorption in the visible light region. Absorption in the visible region indicates that PbTiO_3 nanoparticles have become

visible light active material. It confirms the reduced form of PbTiO₃ on annealing at high temperature in hydrogen atmosphere. Optical band gap of the PbTiO₃ nanoparticles was investigated at room temperature by UV- vis-NIR- spectroscopy. Tauc and Davis Mott model is used to measure the band gap of reduced PbTiO₃ nanoparticles [32].

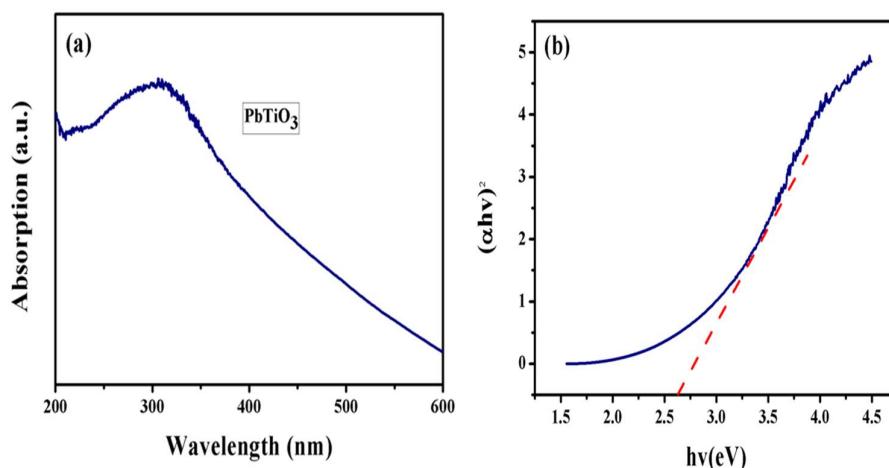


Figure 3. (a) UV-visible spectra for reduced PbTiO₃ nanoparticles, (b) Band gap calculations for reduced PbTiO₃ nanoparticles.

Normally, PbTiO₃ has large band gap (3-4.5 eV) which is active in the UV-light region. Reduced PbTiO₃ induces oxygen vacancies. Each oxygen vacancy provides two free electrons [33]. These free electrons reduce the nearest Ti⁺⁴ to Ti⁺³. Reduction of Ti⁺⁴ to Ti⁺³ induces donor levels just below the conduction band. Formation of these new energy levels inside the band gap causes to reduce the active band gap of PbTiO₃ to 2.65 eV which is active in the visible light region. Figure 3(b) shows the band gap calculation for PbTiO₃ nanoparticles which is estimated to 2.65 eV. In literature band gap of paraelectric cubic PbTiO₃ is reported from 3 to 4.5 eV [23, 24] experimentally while Piskunov *et al.* have reported best calculated band gap 1.7 eV [25]. The band gap value calculated in this work is quite near to the ever best theoretically calculated band gap value, 1.7 eV. Figure 4 represents the schematic diagram for the formation of new energy levels just below the conduction band due to the reduction of Ti⁺⁴ to Ti⁺³.

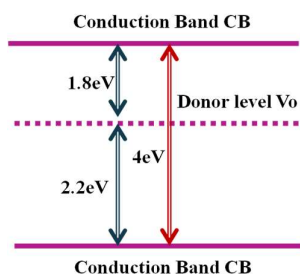


Figure 4. Schematic diagram for PbTiO₃ and reduced PbTiO₃.

Low band gap value of prepared PbTiO_3 nanoparticles makes the material suitable for photocatalytic applications. PbTiO_3 nanoparticles are mostly studied for their piezoelectric effect. Very few reports have been presented for the study of its photocatalytic activity. It has been neglected for a long period of time for its photocatalytic performance because of its large band gap 3 to 4.5 eV [23, 24].

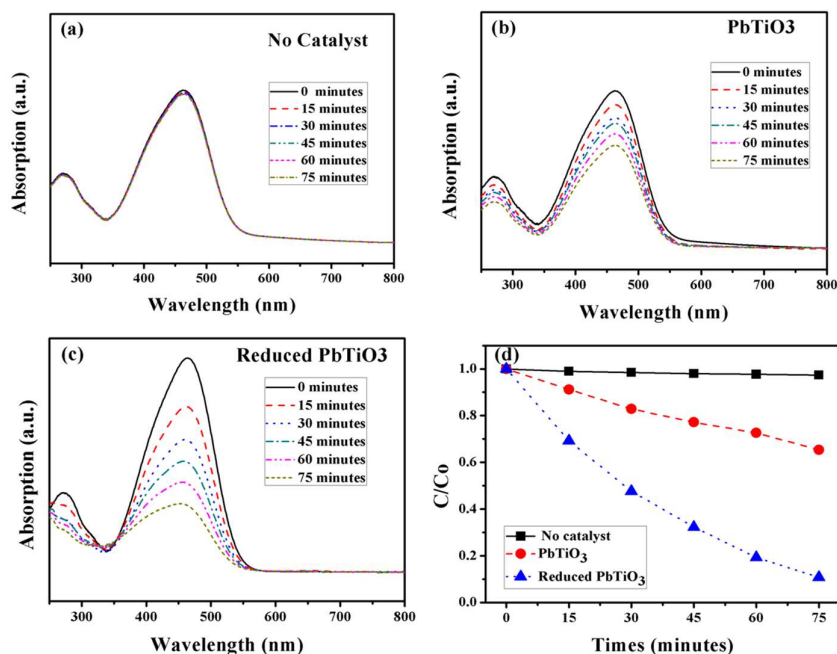


Figure 5. (a) Degradation of MO under solar light without catalyst, (b) with PbTiO_3 , (c) reduced PbTiO_3 and (d) comparison of degradation under different conditions.

Figure 5(a-c) represents the photocatalytic degradation of methyl orange (MO) without catalyst, with PbTiO_3 nanoparticles and reduced PbTiO_3 nanoparticles under solar light irradiation. Figure 5(d) shows the curve of C/C_0 versus time which indicates that methyl orange degraded to 80% within 75 min under solar light irradiation for reduced PbTiO_3 and photocatalytic performance of hydrogenated PbTiO_3 increased due to the formation of new energy levels inside the band gap of PbTiO_3 under solar light irradiation. Photocatalytic performance has improved up to 2.6 times more than that of pure PbTiO_3 nanoparticles.

CONCLUSION

PbTiO_3 nanoparticles are prepared by template free hydrothermal method. Nanoparticles are characterized by XRD, FESEM and EDX. Calculated band gap of PbTiO_3 nanoparticles is nearly 2.65 eV which correspond to the visible region. Low band gap of PbTiO_3 nanoparticles make the material photoactive under visible light which degraded the methyl orange to 80% within 75 min under solar light irradiation and photocatalytic performance of reduced PbTiO_3 improves 2.6 times more than that of pure PbTiO_3 nanoparticles. Such materials can be synthesized and used for photocatalysis as well as water splitting for hydrogen production.

REFERENCES

1. Al-Rasheed, R.; Cardin, D.; Photocatalytic degradation of humic acid in saline waters: Part 2. Effects of various photocatalytic materials. *J. Appl. Cat. A* **2003**, 246, 39-48.
2. Miao, L.; Tanemura, S.; Toh, S.; Kaneko, K.; Tanemura, M. Heating sol gel template process for the growth of TiO₂ nanorods with rutile and anatase structure. *Appl. Surf. Sci.* **2004**, 238, 175-179.
3. Wu, W.P.; Liu, W.C.; Qiu, S.W.; Ma, A.Q.; Dai, W.; Qian, Y. Application of water stable zinc(II) glutamate metal organic framework for photocatalytic degradation of organic dyes. *Bull. Chem. Soc. Ethop.* **2019**, 33, 43-50.
4. Wu, W.P.; Ding, Q.; Wu, X.R.; Huang, Y.J.; Trivedi, M.; Kumar, A. Photocatalytic degradation of organic dyes by infinite one dimensional coordination polymer based on zinc (II) in water. *Bull. Chem. Soc. Ethop.* **2019**, 33, 51-60.
5. Fujishima, A.; Honda, K. Electrochemical photolysis of water at a semiconductor electrode. *Nature* **1972**, 238, 37-38.
6. Choi, W.; Termin, A.; Hoffmann, M.R. The role of metal ion dopants in quantum-sized TiO₂: Correlation between photoactivity and charge carrier recombination dynamics. *J. Phys. Chem.* **1994**, 98, 13669-13679.
7. Chen, L.C.; Chou, T.C. Photodecolorization of methyl orange using silver ion modified TiO₂ as photocatalyst. *Ind. Eng. Chem. Res.* **1994**, 33, 1436-1443.
8. Asahi, R.; Morikawa, T.; Ohwaki, T.; Aok, K.; Taga, Y. Visible-light photocatalysis in nitrogen doped titanium oxide. *Science* **2001**, 293, 269-271.
9. Ohno, T.; Mitsui, T.; Matsumura, M. Photocatalytic activity of S-doped TiO₂ photocatalyst under visible light. *Chem. Lett.* **2003**, 32, 364-365.
10. Tang, Z.R.; Zhang, Y.; Xu, Y.J. Tuning the optical property and photocatalytic performance of titanate nanotube toward selective oxidation of alcohols under ambient conditions. *ACS Appl. Mater. Interf.* **2012**, 4, 1512-1520.
11. Padmanabhan, S.C.; Pillai, S.C.; Colreavy, J.; Balakrishnan, S.; McCormack, D.E.; Perova, T.S.; Gunko, Y.; Hinder, S.J.; Kelly, J.M. A simple sol-gel processing for the development of high temperature stable photoactive anatase titania. *Chem. Mater.* **2007**, 19, 4474-4481.
12. Morikawa, T.; Irokawa, Y.; Ohwaki, T. Enhanced photocatalytic activity of TiO₂-xN_x loaded with copper ions under visible light irradiation. *Appl. Catal. A: General* **2006**, 314, 123- 127.
13. Chen, X.; Liu, L.; Yu, P.Y.; Mao, S.S. Increasing solar absorption for photocatalysis with black hydrogenated titanium dioxide nanocrystals. *Science* **2011**, 331, 746-750.
14. Liu, S.H.; Yang, L.X.; Xu, S.H.; Luo, S.L.; Cai, Q.Y. Photocatalytic activities of C-N-doped TiO₂ nanotube array/carbon nanorod composite. *Electrochem. Commun.* **2009**, 11, 1748-1751.
15. Lai, Y.K.; Huang, J.Y.; Zhang, H.F.; Subramaniam, V.P.; Tang, Y.X.; Gong, D.G.; Sundar, L.; Sun, L.; Chen, Z.; Lin, C.J. Nitrogen-doped TiO₂ nanotube array films with enhanced photocatalytic activity under various light sources. *J. Hazard. Mater.* **2010**, 184, 855-863.
16. Sun, W.T.; Yu, Y.; Pan, H.Y.; Gao, X.F.; Chen, Q.; Peng, L.M. Quantum dots sensitized TiO₂ nanotube-array photoelectrodes. *J. Amer. Chem. Soc.* **2008**, 130, 1124-1125.
17. Yang, L.X.; Chen, B.B.; Luo, S.L.; Li, J.X.; Liu, R.H.; Cai, Q.Y. Sensitive detection of polycyclic aromatic hydrocarbons using CdTe quantum dot-modified TiO₂ nanotube array through fluorescence resonance energy transfer. *Environ. Sci. Technol.* **2010**, 44, 7884-7889.
18. Zhu, W.; Liu, X.; Liu, H.Q.; Tong, D.L.; Yang J.Y.; Peng, J.Y. Coaxial heterogeneous structure of TiO₂ nanotube arrays with CdS as a superthin coating synthesized via modified electrochemical atomic layer deposition. *J. Amer. Chem. Soc.* **2010**, 132, 12619-12626.

19. Wang, M.; Sun, L.; Lin, Z.; Cai, J.; Xie, K.; Lin, C. p-n Heterojunction photoelectrodes composed of Cu₂O-loaded TiO₂ nanotube arrays with enhanced photoelectrochemical and photoelectrocatalytic activities. *Energy Environ. Sci.* **2013**, *6*, 1211-1220.
20. Yang, R.; Yang, L.; Tao, T.; Ma, F.; Xu, M.; Zhang, Z. Contrastive study of structure and photocatalytic performance with three-dimensionally ordered macroporous CuO-TiO₂ and CuO/TiO₂. *Appl. Sur. Sci.* **2014**, *288*, 363-368.
21. Huang, Z.; Wen, X.; Xiao, X. Photoelectrochemical properties of CuS-TiO₂ composite coating electrode and its preparation via electrophoretic deposition. *J. Electrochem. Soc.* **2011**, *158*, H1247-H1251.
22. Hu, S.; Li, F.; Fan, Z.; Gui, J. Improved photocatalytic hydrogen production property over Ni/NiO/N-TiO_{2-x} heterojunction nano composite prepared by NH₃ plasma treatment. *J. Power Source* **2014**, *250*, 30-39.
23. Chen, X.; Fan, H.; Liu, L. Synthesis and crystallization behavior of lead titanate from oxide precursors by a hydrothermal route. *J. Crystal Growth* **2005**, *284*, 434-439.
24. Moret, M.P.; Devillers, M.A.C.; Worhoff, K.; Larsen, P.K. Optical properties of PbTiO₃, PbZr_xTi_{1-x}O₃ and PbZrO₃ films deposited by metalorganic chemical vapor on SrTiO₃. *J. Appl. Phys.* **2002**, *92*, 468-474.
25. Kong, J.Z.; Li, A.D.; Zhai, H.F.; Li, H.; Yan, Q.Y.; Ma, J.; Wu, D. Preparation, characterization and photocatalytic properties of ZnTiO₃ powders. *J. Hazard. Mater.* **2009**, *171*, 49-54.
26. Guan, X.; Guo, L. Cocatalytic effect of SrTiO₃ on Ag₃PO₄ on toward enhanced photocatalytic water oxidation. *ACS Catal.* **2014**, *4*, 3020-3026.
27. Ye, M.; Wang, M.; Zheng, D.; Zhang, N.; Lin, C.J.; Lin, Z. Garden like Perovskite super structures with enhanced photocatalytic activity. *Nanoscale* **2014**, *6*, 3576-3584.
28. Leite, E.R.; Santos, L.P.S.; Carreo, N.L.V.; Longo, E.; Paskocimas, C.A.; Varela, J.A.; Lanciott, F.; Campos, C.E.M.; Pizan, P.S. Photoluminescence of nanostructured PbTiO₃ processed by high energy mechanical milling. *Appl. Phys. Lett.* **2001**, *78*, 2148-2150.
29. Szabo, G.S.; Cohen, R.E.; Krakuer, H. First-principles study of piezoelectricity of PbTiO₃. *Phys. Rev. Lett.* **1998**, *80*, 4321-4324.
30. Piskunov, S.; Heifets, E.; Eglitis, R.I.; Bostel, G. Bulk properties and electronic structure of SrTiO₃, BaTiO₃, PbTiO₃ perovskites: An ab initio HF/DFT study. *Comp. Mater. Sci.* **2004**, *29*, 165-178.
31. Patterson, A.L. The Sherrer formula for X-ray particle size determination. *Phys. Rev.* **1939**, *56*, 978-982.
32. Tauc, J. Optical properties and electronic structure of amorphous Ge and Si. *Mater. Res. Bull.* **1968**, *4*, 37-46.
33. Lin, Y.H.; Liu, Y.S.; Lin, Y.C.; Wei, Y.S.; Liao, K.S.; Lee, K.R.; Lai, Y.; Chen, H.M.; Jean, Y.C.; Liu, C.Y. Decoupling free-carriers contributions from oxygen-vacancy and cation-substitution in extrinsic conducting oxides. *J. App. Phys.* **2013**, *113*, 033706. DOI: 10.1063/1.4776781.